Pergamon

Bioorganic & Medicinal Chemistry Letters 9 (1999) 1613–1618

BIOORGANIC & MEDICINAL CHEMISTRY LETTERS

DESIGN OF SCYTALONE DEHYDRATASE INHIBITORS AS RICE BLAST FUNGICIDES: DERIVATIVES OF NOREPHEDRINE

Gregory S. Basarab,[a,1,*] Douglas B. Jordan,[a] Troy C. Gehret,[a] Rand S. Schwartz,[a] and Zdzislaw Wawrzak[b,2]

[a]*E. I. DuPont de Nemours Agricultural Products, Stine-Haskell Research Center, P.O Box 30, Newark DE, 19714;* [b]*E. I. DuPont de Nemours Life Sciences, Experimental Station, Wilmington DE 19880-0228.*

Received 25 February 1999; accepted 30 April 1999

Abstract. Five X-ray crystal structures of scytalone dehydratase complexed with different inhibitors have delineated conformationally flexible regions of the binding pocket. This information was used for the design and synthesis of a norephedrine-derived cyanoacetamide class of inhibitors leading to potent fungicides.

Previously, we described the design, synthesis, and biological activity of a series of scytalone dehydratase (SD) inhibitors.[3] One of these (**1**, Figure 1) has a K_i = 20 pM against SD and provides excellent control of rice blast disease in outdoor field trials. The X-ray crystal structure of SD with **1** is one of eight SD structures with six different inhibitors that have been reported, together affording a series of snapshots relative to inhibitor structure and protein conformation. The first two reported SD structures were determined from crystals grown under acidic conditions[4,5] that inactivate catalysis and effect a significant reorientation of the Cα atom trace for residues 153-160 relative to more recent structures. The more recent structures were obtained from crystals grown at pH's 7.5–8.0 where the enzyme is optimally active and stable and where physiological conformations are likely represented.[3,6,7] The state of the art for structure-based ligand design involves multiple crystal structures in an iterative optimization process.[8] Here we describe the use of multiple SD crystal structures to identify regions of the protein that undergo structural reorganization that can be exploited for inhibitor and fungicide design.

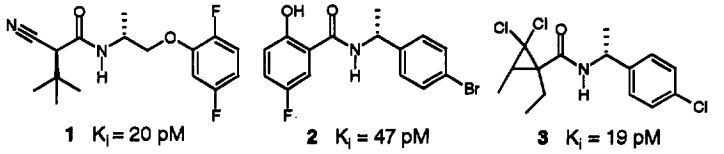

1 K_i = 20 pM **2** K_i = 47 pM **3** K_i = 19 pM

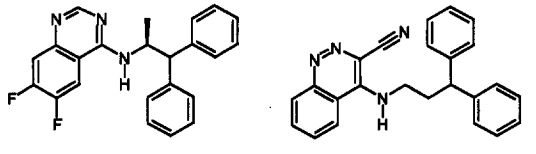

4 K_i = 32 pM **5** K_i = 8 pM

Figure 1. Structures of inhibitors co-crystallized with SD at pH 7.5-8.

0960-894X/99/$ - see front matter
PII: S0960-894X(99)00247-4

Inhibitor design

Figure 1 shows five inhibitors that have been co-crystallized with SD at neutral pH and high resolution for X-ray structure determination.[3,6,7] The structural diversity of the inhibitors (K_i's < 50 pM) demonstrate the promiscuity of the enzyme binding pocket. The structural flexibility of SD becomes apparent when considering that the complexes have the inhibitors buried within requiring opening and closing of the protein for binding. An overlay of the five crystal structures can be used to identify flexible regions of the protein that adapt to the different inhibitors. SD structural flexibility is manifested by a reordering of the binding pocket side chains as opposed to meaningful changes in the Cα atom trace where there is little variation from structure to structure.[7]

Figure 2A shows side chains of eight active site residues that do not move significantly among the five overlaid structures. Inhibitor **1** is included as a frame of reference. The eight residues are affixed to secondary structural elements of the protein that typically have reduced conformational flexibility: three α-helices (residues 13–31, 63–70, and 162–171) and three long anti-parallel strands (residues 81–96, 99–113, and 123–138) that form a β-sheet. Among these more static residues are Tyr30, His85, His110, and Asn131, which are important recognition elements for **1** and which exhibit positional rmsd's ranging from 0.3–0.7 Å.[9] From a design point of view, it follows that modifications of an inhibitor to extend into the space of these more static residues would very likely be deleterious to binding potency.

Binding site residues that move to accommodate the five inhibitors contact the lipophilic nitrogen substituents of the inhibitors (Figure 2B), and their capability to mesh with the inhibitors is part of the molecular recognition dynamics. Phe53, which resides at the apex of a loop that has been demonstrated to offer a measure of conformational flexibility,[7] displays the greatest positional variation among the binding site residues with an rmsd of 2.9 Å.[9] In the SD complex with **1**, Phe53 points edgewise to the methylene of the three-atom bridge connecting the carboxamide nitrogen atom to the phenyl group while the π-face borders one of the *t*-butyl methyl groups. Substitution for the methylene pro-*S* hydrogen atom would overlap Phe53 compelling the residue

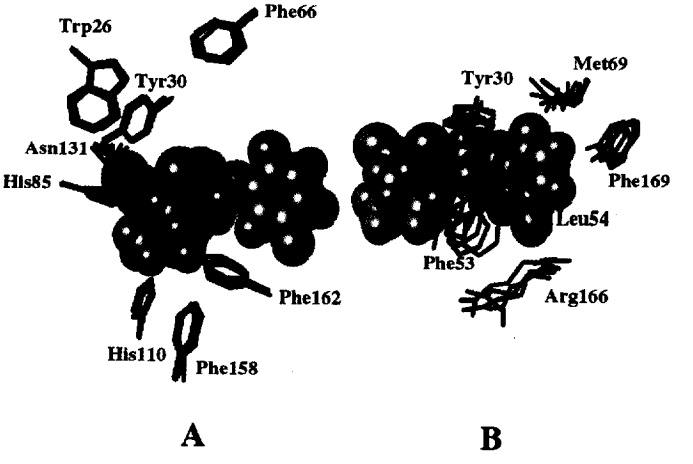

Figure 2. Crystal Structure Comparisons.

(A) Static side chains from five SD-inhibitor complexes relative to compound **1** (green, spacefill).

(B) Mobile side chains from five SD-inhibitor complexes relative to compound **1** (green, spacefill).

to move outward. A phenyl substituent was favored due to the potential for π-π stacking with Phe53.[10] However, the SD crystal structure conformation of **1** reveals that substitution for the pro-*S* hydrogen suffers from an unfavorable intramolecular steric overlap with the methyl of the *t*-butyl group that points into the Phe53 π-face. To accommodate the phenyl substituent, the *t*-butyl group must be reduced in size. Doing so also compensates for the additional lipophilicity imparted by the phenyl substituent, which is important for maintaining favorable physical properties for expression of in vivo activity. Norephedrine contains the desired absolute configuration with phenyl substitution at the pro-*S* position and serves as a readily available chiral building block for synthesis.

Chemistry

Four cyanoacetyl chlorides were made from the known ethyl,[11] cyclopropyl,[12] isopropyl,[13] and *t*-butyl[14] substituted acetic acids. The acid chlorides were reacted with (*R*)-2,5-difluorophenoxypropyl amine[3] to afford 1:1 mixtures of epimers due to the asymmetric center on cyanoacetic acid portion of the molecules (Scheme 1).

Scheme 1.

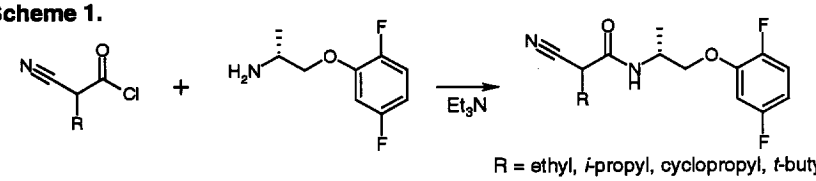

In the inhibition model we developed, the norephedrine absolute *R,S* stereochemistry had to be maintained in the final products. Arylation of norephedrine with *o*-fluorobenzonitriles was achieved with sodium hydride as base and without protecting group chemistry in 60-70% yield. The product amino ethers required no further purification except for the reaction with 2,4-difluorobenzonitrile in which a chromatographically separable 2:1 mixture of *ortho* to *para* fluoride displacement products was obtained (Scheme 2). Subsequent acylation with substituted cyanoacetyl chlorides afforded inhibitors **7a–7g** (Table 1).

Structure–activity correlations around **1** demonstrate 2,5-difluoro substitution to be ideal,[3] thus requiring an alternate synthetic route. Norephedrine was converted in three steps to the aziridine (Scheme 3), which was opened with phenoxide to afford predominately the desired benzyl ether. Removal of the phosphonyl group with

Scheme 2.

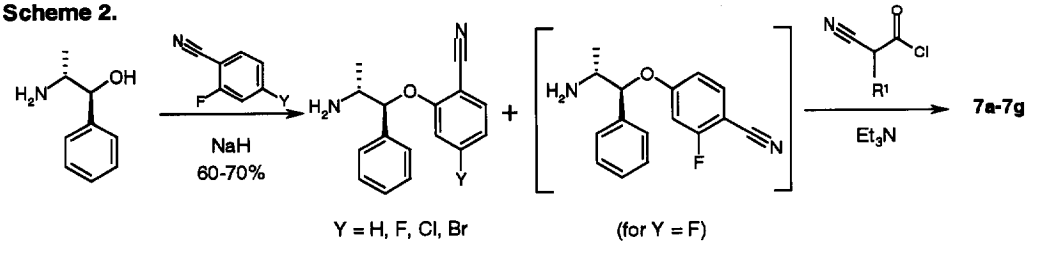

Scheme 3.

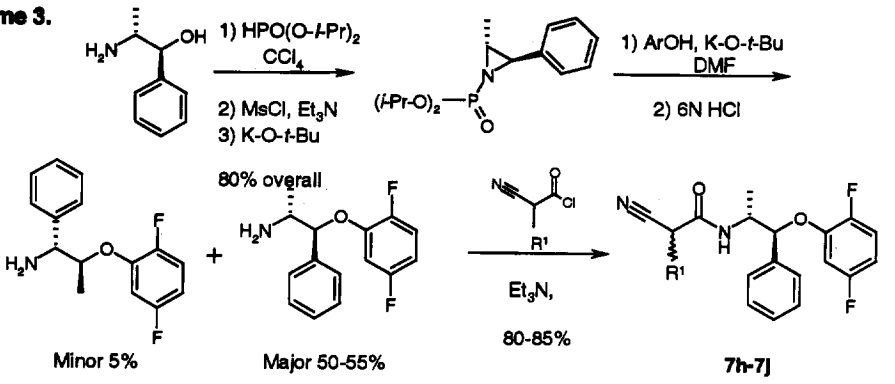

acid gave the requisite amine for subsequent acylation. The phosphonyl group serves well as a protecting and activating group for double inversion of stereochemistry at the benzylic carbon as required by our design.

Results and Discussion

Table 1 summarizes the SD inhibition data and greenhouse activity for the series of inhibitors, each synthesized as a 1:1 epimeric mixture. K_i's[6] and greenhouse disease control data[15] were determined as described. ED_{90} represents the compound concentration that affords 90% control of blast disease on rice plants in a greenhouse assay as determined from dose responses. For the difluorophenoxypropyl derivatives **6a–6d**, SD inhibitory potency increases as R^1 increases in size. This trend primarily reflects the increase in lipophilicity that accompanies larger R^1 substituents although there may be small contributions to binding from increases in van der Waals contact surface area. The foliar rice blast disease control (ED_{90}) correlates well with K_i.

The trend for the R^1 substituent of norephedrine derivatives **7a–j** differs considerably from that seen for compounds **6a–d** in that the *t*-butyl substituent is less active versus SD than the ethyl, isopropyl or cyclopropyl group (compare **7g** with **7a** and **7e**). Comparison of **6a** with **7h** is particularly noteworthy in that the additional phenyl group increases SD inhibitory potency nearly 300-fold and markedly improves greenhouse efficacy. Though the isopropyl group approaches ethyl in potency versus SD for the norephedrine derivatives, it reduces the expression of activity in greenhouse assays (compare **7h** and **7j**) due to there being a small window of lipophilicity that can be tolerated for systemic movement in the plant.[16] Compound **7i** with the cyclopropyl group exhibits the greatest inhibitory potency. Compound **7h** with the ethyl group along with **7i** performs best in greenhouse assays. The 2,5-difluoro substitution pattern affords the highest activity in the foliar assay represented in Table 1 and in a number of other greenhouse assays (data not shown).

To validate the design concept for these norephedrine derivatives, the X-ray structure of SD complexed with **7a** was solved to 1.9 Å resolution using reported methods for crystallization, data collection and refinement.[6,7,17] The electron density map was excellent both around the inhibitor and the enzyme binding pocket. Since **7a** is a 1:1 mixture of epimers, the enzyme selects the better binding isomer, which was determined to have

Table 1. Inhibition and Greenhouse Efficacy for Norephedrine Derivatives

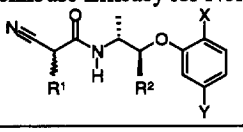

Compound	R^1	R^2	X, Y	K_i (pM)	ED_{90} (mg/L)
6a	ethyl	H	F, F	5500 ± 130	>200
6b	cyclopropyl	H	F, F	1100 ± 44	50
6c	isopropyl	H	F, F	270 ± 31	10
6d	*tert*-butyl	H	F, F	42 ± 6	6
7a	ethyl	phenyl	CN, H	70 ± 5	10
7b	ethyl	phenyl	CN, F	21 ± 5	50
7c	ethyl	phenyl	CN, Cl	31 ± 1	10
7d	ethyl	phenyl	CN, Br	34 ± 5	50
7e	isopropyl	phenyl	CN, H	38 ± 4	25
7f	isopropyl	phenyl	CN, F	34 ± 3	25
7g	*tert*-butyl	phenyl	CN, H	140 ± 6	200
7h	ethyl	phenyl	F, F	20 ± 2	2
7i	cyclopropyl	phenyl	F, F	14 ± 2	2
7j	isopropyl	phenyl	F, F	76 ± 2	100

the absolute *R* configuration (the same as that for **1**[3]) for the cyanoacetic acid portion of the molecule. As in previously reported X-ray structures of SD-inhibitor complexes, there are two water molecules associated with the carboxamide of **7a**. The Cα atoms for the SD complex with **7a** have an rmds of 0.3 Å relative to the complex with **1**. The greatest deviation in the Cα atoms occurs in the loop region encompassing residues 50-55 where there was as much as a 1.0 Å outward movement in the **7a**–SD complex. The enzyme conforms to the additional phenyl group of **7a** relative to **1** with this outward movement, a concomitant 1–3 Å displacement of the Phe53 atoms and a rotation away from the binding pocket of the side chain of Arg166. The phenyl group of Phe53 lies nearly parallel to the phenyl group of **7a** with a plane angle of 23° and forms an edge-to-edge perpendicular interaction with the phenoxy group with a plane angle of 106°.

Binding enhancements imparted by the R^2 phenyl of the norephedrine derivatives result from the entropic effect due to increased lipophilicity and from the increased surface area for van der Waals contacts. Furthermore, the additional asymmetric center on the flexible phenoxypropyl chain limits the degrees of rotational freedom by favoring non-eclipsing interactions thereby offering another entropic advantage to binding. Figure 3 shows the overlays of **7a** and **1** determined from their respective crystal structures. The overlays were generated by mapping protein Cα atoms onto corresponding protein Cα atoms, so there is no bias in the alignments from the inhibitors themselves. It is clear that the *t*-butyl group of **1** would not be tolerated in **7a** without significant conformational changes in both the inhibitor and the protein. The observed retention of location and geometry of the two inhibitors in their respective crystal structures proves that a conformationally flexible region of the enzyme was correctly identified, thus allowing incorporation of the phenyl substituent.

In summary, a series of cyanoacetamide derivatives of norephedrine were designed from insights gleaned from comparisons of SD crystal structures. The synthesized molecules are highly potent inhibitors of SD and perform well in plant disease control evaluations. The concept of the design was further validated with an X-ray crystal structure of one inhibitor in complex with SD. One of the unmet challenges for structure-based design is anticipating protein conformational changes in response to ligands. Multiple X-ray structures in iterative design programs will continue to contribute towards delineating the nature of conformational changes that are important for understanding the dynamics of molecular recognition.

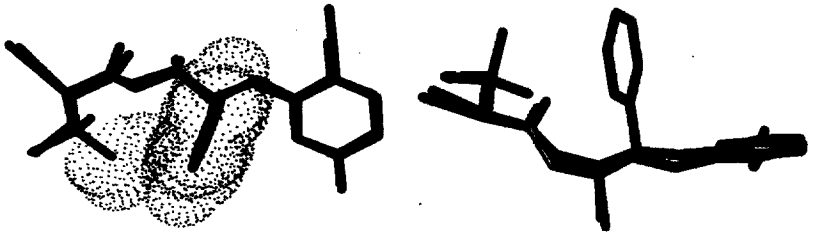

Figure 3. Top and side views of the overlay of compounds **1** (red) and **7a** (blue) from the complexes with SD. Included on the left are overlapping van der Waals dot surfaces (methyl of **1** and phenyl of **7a**).

References and Notes

1. Present address: E. I. DuPont de Nemours Life Sciences, Bldg. 328, Experimental Station, Wilmington, DE 19880-0328.
2. Present address: Northwestern University, DND-CAT, 9700 S. Cass Ave., Argonne, IL 60439.
3. Jordan, D. B.; Lessen, T.; Wawrzak, Z.; Bisaha, J. J.; Gehret, T. C.; Hansen, S. L.; Schwartz, R. S.; Basarab, G. S. *J. Bioorg. Med. Chem. Lett.* **1999**, *9*, 1607.
4. Lundqvist, T.; Rice, J.; Hodge, C. N.; Basarab, G. S., Pierce, J.; and Lindqvist, Y. *Structure (London)* **1994** *2*, 937.
5. Nakasako, M.; Motoyama, T.; Kurahashi, Y.; Yamaguchi, I. *Biochemistry* **1998**, *37*, 9931.
6. Chen, J. M.; Xu, S. L.; Wawrzak, Z.; Basarab, G. S.; Jordan, D. B. *Biochemistry* **1998**, *37*, 17735.
7. Wawrzak, Z.; Sandalova, T.; Steffens, J. J.; Basarab, G. S.; Lundqvist, T.; Lindqvist, Y.; Jordan, D. B. *Proteins: Struct., Funct. Genet.*, in press.
8. Babine, R. E.; Bender, S. L. *Chem. Rev.* **1997**, *97*, 1359.
9. Rmsd's (root mean squared deviations) were determined from distances between the residues atoms in the SD complex with **1**, **3**, **4** and **5** and the identical atoms in the SD-**2** complex after alignment of Cα atoms.
10. Hunter, C. A.; Sanders, J. K. M. *J. Am. Chem. Soc.* **1990**, *112*, 5527.
11. Winters, G.; Di Mola, N.; Oppici, E.; Nathansohn, G. *Farmaco Ed. Sci.* **1975**, *30*, 620.
12. Carney, R. W. J.; Wojtkunski, J. *Org. Prep. Proced. Int.* **1973**, 5, 25.
13. Cativiela, C.; Diaz-de-Villegas, M. D.; Galvez, J. A. *J. Org. Chem.* **1994**, *59*, 2497.
14. Schawmann, E.; Mrotzek, H. *Tetrahedron* **1979** *35*, 1965.
15. Basarab, G. S.; Hansen, S. L.; Jordan, D. B.; Lessen, T. A. Pct. Int. Appl. WO 9833765 A1, 1998; *Chem. Abstr.* **1998**, *129*, 175444.
16. Bromilow, R. H.; Chamberlain, K. *Monogr. - Br. Plant Growth Regul. Group* **1989**, *18*, 113.
17. Details of the X-ray structure will be presented elsewhere.